Influence of a NH_2-terminal extension on the activity of KTX2, a K^+ channel blocker purified from *Androctonus australis* scorpion venom

Christian Legros, Eric Feyfant, François Sampieri, Hervé Rochat, Pierre E. Bougis, Marie-France Martin-Eauclaire*

Laboratoire de Biochimie, Ingénierie des Protéines, UMR 6560 du Centre National de la Recherche Scientifique, Institut Fédératif Jean Roche, Faculté de Médecine Nord, Boulevard Pierre Dramard, 13916 Marseille Cedex 20, France

Received 16 August 1997

Abstract A cDNA encoding a short polypeptide blocker of K^+ channels, kaliotoxin 2 (KTX2), from the venom of the North African scorpion *Androctonus australis* was expressed in the periplasmic space of *Escherichia coli*. KTX2 was produced as a fusion protein with the maltose binding protein followed by the recognition site for factor Xa or enterokinase preceding the first amino acid residue of the toxin. The fully refolded recombinant KTX2 (rKTX2) was obtained (0.15–0.30 mg/l of culture) and was indistinguishable from the native toxin according to chemical and biological criteria. An N-extended analogue of KTX2 exhibiting three additional residues was also expressed. This analogue had 1000-fold less affinity for the ^{125}I-kaliotoxin binding site on rat brain synaptosomes than KTX2. Conformational models of KTX2 and its mutant were designed by amino acid replacement using the structure of agitoxin 2 from *Leiurus quinquestriatus* as template, to try to understand the decrease in affinity for the receptor.

Key words: Scorpion toxin; Potassium channel; Heterologous expression; *Escherichia coli* periplasm

1. Introduction

Efforts to characterise minor components in scorpion venoms have led to the discovery of short toxins (31–40 amino acids residues, three disulphide bridges) able to act on different types of K^+ channels [1,2]. The diversity of K^+ channels is large [3,4] and there has been a profusion of research for new selective ligands in order to elucidate their mechanisms of action and pharmacological significance. A K^+ channel blocker, kaliotoxin (KTX), has been characterised from the venom of the Moroccan scorpion *Androctonus mauretanicus*; KTX is a single 4-kDa polypeptide chain (38 amino acid residues, three disulphide bridges) which acts on the intermediate conductance Ca^{2+}-activated K^+ channel in invertebrate neurons (IKCa) and on voltage-dependent K^+ channels (Kv) of the mammalian nervous system [5,6]. A new KTX-like peptide, KTX2, was isolated from the venom of the North African scorpion *Androctonus australis* [7]. It is a 37-amino acid residue peptide, with a non-amidated COOH-terminus, which displays 76% sequence identity with KTX. KTX and KTX2 differ by their N-terminal portion and also by the replacement of His^{34} and Arg^{31} in KTX by Asp and Gly in KTX2. These two residues are located in the COOH-terminal region which is highly conserved among 'short toxins' active on K^+ channels and which has been assumed to be involved in the interaction with the pore of the channel [8–11]. Most of the conserved amino acid residues are located in an antiparallel β-sheet made of two short strands connected by a turn [12,13]. To obtain enough material for structural and additional biological studies of KTX2, it was necessary to produce the toxin by chemical synthesis or in heterologous expression systems. The cDNA of KTX2 has already been obtained from a cDNA library of *A. australis* venom glands [7,14], by polymerase chain reaction (PCR), using degenerate primers targeted against the highly conserved amino acid cluster. It is a 370-bp cDNA, encoding the KTX2 precursor which is constituted of a signal peptide (22 amino acid residues) followed by the mature KTX2. We used this cDNA to produce a recombinant KTX2 (rKTX2), directly addressed as fusion protein to the periplasmic space of *Escherichia coli*, as well as an NH_2-extended mutant exhibiting 1000-fold less affinity for its receptor site on rat brain synaptosomes.

2. Materials and methods

2.1. Materials

Synthetic KTX (sKTX) was synthesised by. Dr Romi in the laboratory according to [6]. Specific antibodies against sKTX were obtained in rabbit [7]. Restriction and DNA modifying enzymes were purchased from Boehringer Mannheim. [α-^{35}S]dATP used for nucleotide sequencing and ^{125}I-K for radiolabelling of KTX were from Amersham. pMAL-p, 6220 bp, was from Biolab. UV-grade acetonitrile was from Fisons Scientific, trifluoroacetic acid was from Baker. Other solvents and reagents were analytical grade commercial products from Sigma and Merck. The water used to prepare solvents and buffers was obtained with the Milli/Ro/Milli Q system from Millipore.

2.2. Construction of the recombinant KTX2 gene

The template used for PCR was the double strand cDNA of KTX2 [7] inserted into pBluescript SK^+ (Stratagene). Oligonucleotide primers were synthesised on an Applied Biosystems 381A DNA synthesiser. They were as follows: constructions 1 and 2: 5′ AAA ATC CAC GTG AGA ATT CCA GTG TCA TGT 3′ as forward primer containing a *Pml*I restriction enzyme site (underlined) and corresponding to positions 77–99 of the KTX2 cDNA, i.e. NH_2-terminal residues 1–7 of KTX2; construction 3: 5′ GAA AGG CCT GAT GAC GAT GAC AAG GTG AGA ATT CCA GTG TCA TGT 3′ as forward primer carrying a *Stu*I restriction enzyme site (underlined) and corresponding to five codons encoding an enterokinase cleavage site and positions 77–99 of the KTX2 cDNA, i.e. NH_2-terminal residues 1–7 of KTX2. For the three different constructions, the reverse primer 5′ AAA CTG CAG TCA CTT TGG TGT ACA ATC GCA 3′ was used carrying a *Pst*I restriction enzyme site (underlined) and corresponding to positions 192–171 of KTX2 cDNA, i.e. the stop codon and COOH-terminal residues 37–32 of KTX2.

2.3. PCR

PCR was performed and the PCR products were visualised as de-

*Corresponding author. Fax: (33) 04 91 69 88 39.

PII S0014-5793(97)01177-0

scribed [7]. The band with the appropriate size was recovered, purified using the Wizard PCR Prep DNA Purification System (Promega) according to the manufacturer's instructions and reamplified by a second PCR reaction in the same conditions.

2.4. Sequence analysis of the constructions

The purified PCR products were filled in with dNTPs using the Klenow fragment according to standard methods [15], digested with restriction enzymes corresponding to the restriction sites at the 5'-ends of both primers and ligated into the vector pMAL-p. *E. coli* DH5α was used for plasmid propagation. Transformants containing the correctly constructed DNA fragments were analysed by restriction digest with *Eco*RV and *Nsi*I using standard techniques [15] and sequenced with Sequenase (Amersham) using the Sanger dideoxynucleotide chain termination method [16] according to the supplier's instructions.

2.5. Production of fusion proteins and purification by affinity chromatography

E. coli strain DH5α (BRL) carrying the gene fusions was grown at 37°C in Circle Grow medium (Bio-101) containing 50 μg/ml ampicillin. When the cell density had reached A_{600}=0.5, induction was initiated by the addition of 0.2 mM isopropyl β-D-thiogalactoside (IPTG). Cells were harvested 3 h after addition of IPTG and periplasmic extracts prepared by osmotic shock [17]. The periplasmic extracts (400 ml) were applied to an amylose affinity resin (2.5×7 cm column) in 20 mM Tris-HCl, 0.2 mM NaCl, 1 mM EDTA buffer, pH 7.4. After elution of the unbound proteins (the optical density of the eluant being around 0.02), the bound maltose binding protein (MBP)-KTX2 fusion protein was eluted from the amylose resin in the same buffer containing 10 mM maltose. Then, the MBP-KTX2 was desalted using Microsep microconcentrators (Filtron Technology Corporation) with a 10 K cutoff.

2.6. Polyacrylamide gel electrophoresis

SDS-PAGE of proteins was performed on 12% Phast-Gel (Phast-System, Pharmacia) and gels were stained with silver according to the manufacturer's instructions.

2.7. Slot blots

Nitrocellulose membrane (Bio-Rad Laboratories) were used for slot blots according to the protocol supplied with the Bio-Rad Immuno-Blot assay kit anti-rabbit IgG alkaline phosphatase conjugate. The anti-KTX serum was used at a 10^4-fold dilution.

2.8. Cleavage of MBP-KTX2 fusion protein

Various conditions for cleavage of the MBP-KTX2 (obtained with construction 1) and MBP-KIH-KTX2 (obtained with construction 2) by factor Xa (three different sources: Boehringer, Sigma, Bachem) were tried: fusion proteins (concentration of 1 mg/ml, 35 μg/assay) were incubated in 20 mM Tris-HCl, 100 mM NaCl and 2 mM $CaCl_2$ buffer, pH 8, at different ratios of factor Xa to the fusion proteins (3–15% mass/mass), for different times and at various temperatures (24 h or 48 h at 4°C, 26°C or 37°C). To increase the cleavage yield, guanidine chlorohydrate (0.1–1 M), urea (0.1–1 M), SDS (0.1–1%), acetonitrile (10% v/v) or guanidine chlorohydrate+acetonitrile, urea+acetonitrile, SDS+acetonitrile (amounts as above) were added. To cleave the MBP-KTX2 (obtained with construction 1), factor Xa was also replaced by trypsin or arginine C-protease (Sigma) in the same conditions. To cleave MBP-KTX2 (obtained with construction 3) bovine enterokinase (two different sources: Sigma, Biozyme; 3–15% mass/mass) was used in 50 mM Tris-HCl, 5 mM $CaCl_2$, pH 8 or pH 5.2 with acetonitrile (10% v/v) at 26°C for 24 h. Guanidine chlorohydrate, urea, SDS (amounts as described above) were also added to the samples to increase the cleavage yield.

2.9. High performance liquid chromatography (HPLC)

The recombinant toxins were purified by reverse-phase HPLC at 25°C on a Merck (4×250 mm) analytical column prepacked with 5 μm of Lichrospher 100 RP-18 on a Waters Associates system as previously described [5]. HPLC on an anionic exchanger (DEAE-3SW Spherogel TSK column from Beckman, 7.5×7.5 mm) was also performed (solvent A, water, solvent B, 1 M ammonium acetate, pH 7.6). Detailed descriptions of all the chromatographic steps are given in the text and figure legends. Samples for biological assays were lyophilised in the presence of 0.1% BSA.

2.10. Protein chemistry

2.10.1. Amino acid sequence. An Applied Biosystems 476A sequencer and the recommended program cycles were used for automated Edman degradation. Phenylthiohydantoin derivatives were characterised by HPLC as described [7].

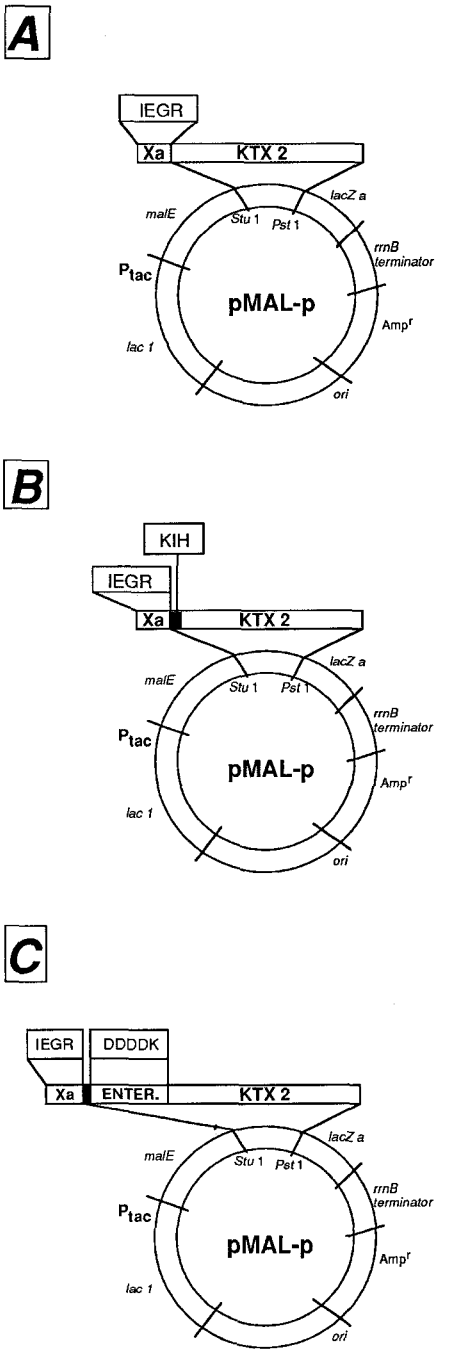

Fig. 1. Schematic diagram of plasmid pMAL-p constructions used for the production of MBP-KTX2 and MBP-KIH-KTX2. A: pMAL-p-(fac.Xa)-KTX2. B: pMAL-p-(fac.Xa)-KIH-KTX2. C: pMAL-p-(fac.Xa-EnK)-KTX2. Three ligations were performed using the 6.2-kbp *Stu*I-*Pst*I fragment of pMAL-p (downstream of the *malE* gene) and (A) the 124-bp *Pml*I-*Pst*I PCR fragment containing the region encoding mature KTX2; (B) the 133-bp *Pml*I-*Pst*I PCR product encoding the KIH-KTX2 peptide; (C) the 139-bp *Stu*I-*Pst*I PCR fragment encoding KTX2 downstream of the enterokinase cleavage site.

2.10.2. Mass spectrometry. Electrospray mass spectrometry of the recombinant KTX2 was performed by Neosystem as already described [7].

2.11. Radioiodination of sKTX

His[34] in synthetic KTX was radiolabelled using Iodogen as already described [7]. Specific radioactivities of 2000 Ci/nmol were routinely obtained. The radioactivity was counted using a Packard Crystal II multidetector system spectrometer.

2.12. Competition binding assay on rat brain synaptosomes

Assays were performed on the synaptosomal fraction P2 from rat brain as previously described [6]. See also figure legends for experimental detail.

2.13. Modelling

Homology modelling was performed on a Silicon Graphics R3000 Indigo workstation using MODELLER [18]. Target (KTX2 or KIH-KTX2) and template (agitoxin 2, AgTX2) [19] sequences were automatically aligned by MODELLER, which subsequently generated the coordinates of both models. Successive energy minimisations and simulated annealing cycles were run, taking into account a set of constraints including probability density functions compiled from the template structures and from a set of reference protein structures [18]. Hydrogen atoms were generated on the final models which were briefly energy-minimised, with all backbone atoms constrained. Models were checked with PROCHECK [20] for geometry compliance.

3. Results

Our first aim was to obtain a fully active recombinant KTX2. Due to the existence of several potential tryptic cleavage sites in the KTX2 molecule (R_2, R_{23}, K_{26}, K_{31}), it was necessary to use highly selective enzymatic conditions. BrCN cleavage from a fusion protein including MBP and KTX2 was also impossible because of the presence of M_{22} and M_{28}. The factor Xa cleavage site and also an enterokinase site were therefore used.

3.1. Construction of the expression vectors and expression of the fusion proteins

The cDNA encoding KTX2 was amplified by PCR with non-degenerate forward and reverse primers. The non-coding regions and the signal peptide of the toxin were removed from the cDNA and specific restriction enzymes sites were added to facilitate insertion into the pMAL-p expression vector, such that a gene fusion could be constructed. There is a *Sac*I, *Kpn*I, *Eag*I, *Bam*HI polylinker between the *malE* gene and the oligonucleotides encoding the factor Xa cleavage site, 5′ to a *Stu*I site. Three different constructions were made (Fig. 1). In the first construction, the KTX2 sequence was inserted between the *Stu*I and the *Pst*I sites, downstream of the sequence encoding the factor Xa cleavage site located at the 3′ end of the *malE* gene (Fig. 1A). Due to a failure of *Pml*I to cleave all the amplified PCR product before its insertion into pMAL-p, an additional construction was found by sequence analysis of the different products. This fortuitous construct contained three codons encoding the amino acid sequence

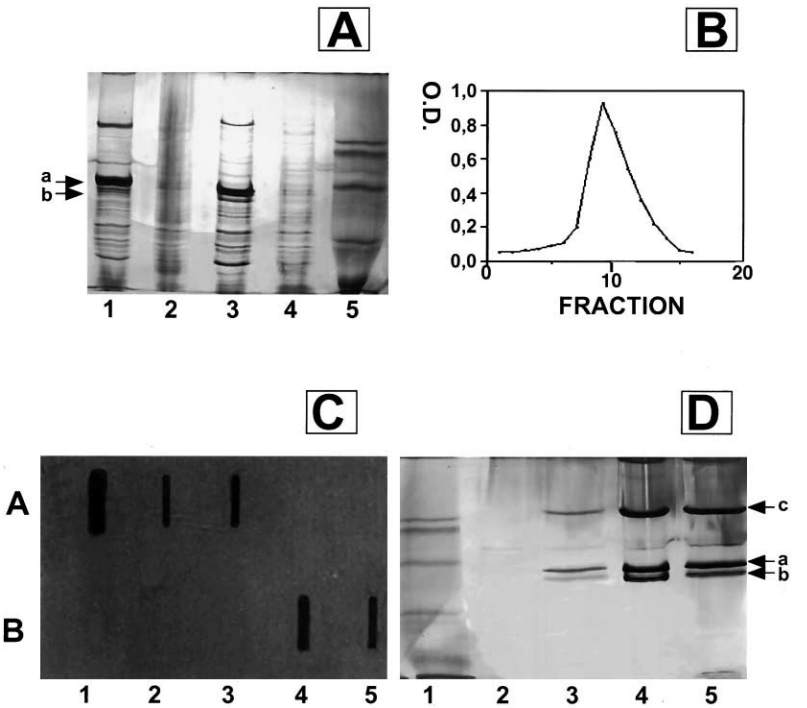

Fig. 2. Characterization of MBP-KTX2. A: SDS-PAGE of periplasmic extracts from non-induced and IPTG-induced *E. coli* cells carrying the MBP-KTX2 gene fusion. Lanes 1 and 2, induced and non-induced cells harbouring construction 1 (data not shown for constructions 2 and 3, but similar results were obtained); lanes 3 and 4, induced and non-induced cells harbouring pMAL-p as control; lane 5, molecular weight markers; arrows indicate: a, MBP-KTX2; b, MBP. B: Purification of MBP-KTX2 using maltose and an amylose affinity column. Amylose column (2.5×7 cm) in 20 mM Tris-HCl, 0.2 mM NaCl, 1 mM EDTA buffer, pH 7.4; flow rate 20 ml/h; 400 ml of periplasmic extract each time; when the flow-through reached OD 0.02 at 280 nm, elution buffer containing maltose was added; fractions of 2 ml were collected. C: Slot blots of the affinity-purified proteins and controls. Lane A, 1, 2, 3, sKTX as positive control (respectively 1 μg, 0.1 μg, 10 ng); 5, synthetic peptide (10 μg) as negative control; Lane B, 1, 2, α-scorpion toxin as negative control (respectively 1 μg, 0.1 μg); 4, 5, MBP-KTX2 (respectively 4 μg, 0.4 μg); the anti-sKTX serum was used at a 10^4-fold dilution and revealed using an anti-rabbit IgG-alkaline phosphatase conjugate. D: Analysis on SDS-PAGE of the affinity-purified proteins after silver staining. Lane 1, molecular weight markers; lanes 2, 3, 4 and 5, respectively fractions 6 (baseline), 7, 8, 9 (top) purified in B. Arrows indicate: a, monomeric form of MBP-KTX2; b, MBP; c, dimeric form of MBP-KTX2.

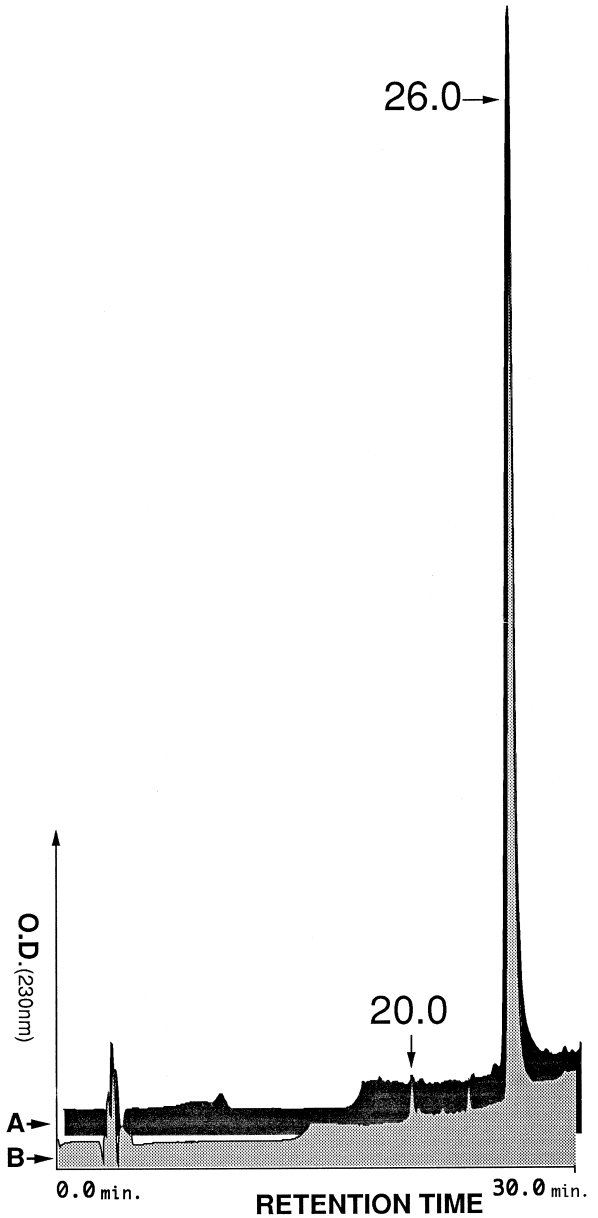

Fig. 3. Purification of rKTX2. RP-C18 column; solvent A, 0.1% TFA; solvent B, acetonitrile+0.1% TFA; linear gradient from 5% to 80% of B in A during 25 min, followed by an isocratic step at 80% of B in A; flow rate 1 ml/min; absorbance was monitored at 230 nm with a 1 Optical Density Unit Full Scale. Chromatogram A: digest of construction 1 with factor Xa (40 μg of MBP-KTX2); chromatogram B: digest of construction 2 with enterokinase (40 μg of MBP-KTX2); rKTX2 eluted at 20 min and MBP-KTX2 at 26 min.

KIH in frame between the factor Xa and KTX2 sequences and thus encoded a KTX2 mutant with three additional residues at its NH_2-terminus (Fig. 1B). In the third construction, five codons encoding an enterokinase cleavage site (DDDDK) were added at the blunt-end *Stu*I restriction site 5′ to the factor Xa sequence such that the linker between MBP and KTX2 in the fusion was IEGRPDDDDK (Fig. 1C). These various constructs were used to transform *E. coli* and were expressed upon IPTG induction. Periplasmic extracts (before and after induction) of the transformants and of cells containing pMAL-p as controls were subjected to SDS-PAGE (Fig. 2A). Intense bands corresponding to the molecular weights of the expected proteins were obtained: 40 kDa for MBP and 44 kDa for MBP-KTX2. Large-scale cultures (1 l) of the transformants were grown, induced with IPTG and the periplasmic extracts prepared 3 h later. MBP derivatives were then purified from these extracts on an amylose affinity column as explained in Section 2 (Fig. 2B). The yields of affinity-purified proteins were 15–20 mg/l of culture, estimated by absorbance at 280 nm. The purified material was desalted and concentrated, then analysed by dot blots (Fig. 2C). No specific antibodies against natural KTX2 were available. Thus, specific antibodies against sKTX were used for blotting experiments. These antibodies were previously unable to recognise native KTX2 in liquid RIA [7], in spite of high sequence similarities between the two toxins (76%). This suggested that conformational epitopes were preferentially recognised in solution as already demonstrated with long α-scorpion toxins [21]. Analyses with synthetic peptides derived from KTX indicated that, in liquid RIA, the 12 NH_2-terminal residues, which differed from those of KTX2, are important for antibody recognition [7]. Immunoblot experiments were performed with sKTX as positive control, MBP-KTX2, and a long α-scorpion toxin and a synthetic peptide as negative controls. This synthetic peptide (12 amino acids residues) was designed according to the N-terminal sequence of a novel toxin acting on K^+ channels (unpublished) and was not expected to react with the anti-sKTX antibodies. As expected, the α-scorpion toxin and the synthetic peptide were not recognised by the anti-sKTX antibodies. However, MBP-KTX2 bound these antibodies, indicating that the fusion contained sKTX epitopes. Analysis of the affinity-purified proteins by SDS-PAGE showed three major bands (Fig. 2D): one at 40 kDa corresponding to MBP (probably due to deletion of the insert during the culture), one at 44 kDa corresponding to MBP-

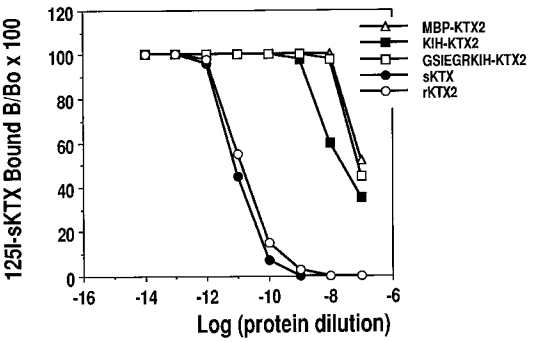

Fig. 4. Competition experiments for binding to rat brain synaptosomal fraction. Membranes (30 μg/assay) in 25 mM Tris-HCl, pH 7.4, 50 mM NaCl, 0.1% BSA were incubated for 1 h at 26°C with ^{125}I-sKTX (40 pM final concentration) and each of a series of concentrations of protein to test. The experiment was stopped by centrifugation at 11 000×*g* for 5 min. The membrane pellets were washed twice with 1 ml of cold washing buffer (20 mM Tris-HCl, 150 mM NaCl, 0.1% BSA, pH 7.4) and the radioactivity bound to the membrane was counted. B_0 is the binding of ^{125}I-sKTX in the absence of competitor and B is the binding in the presence of the indicated concentrations of sKTX (●), rKTX2 (○), rKIH-KTX2 (■), rGSIEGRKIH-KTX2 (□) or MBP-KTX2 (△). Non-specific binding determined in the presence of 0.1 μM sKTX was about 25%. Data points correspond to duplicates from which non-specific binding has been subtracted. The standard error of the mean of the data was around 5%.

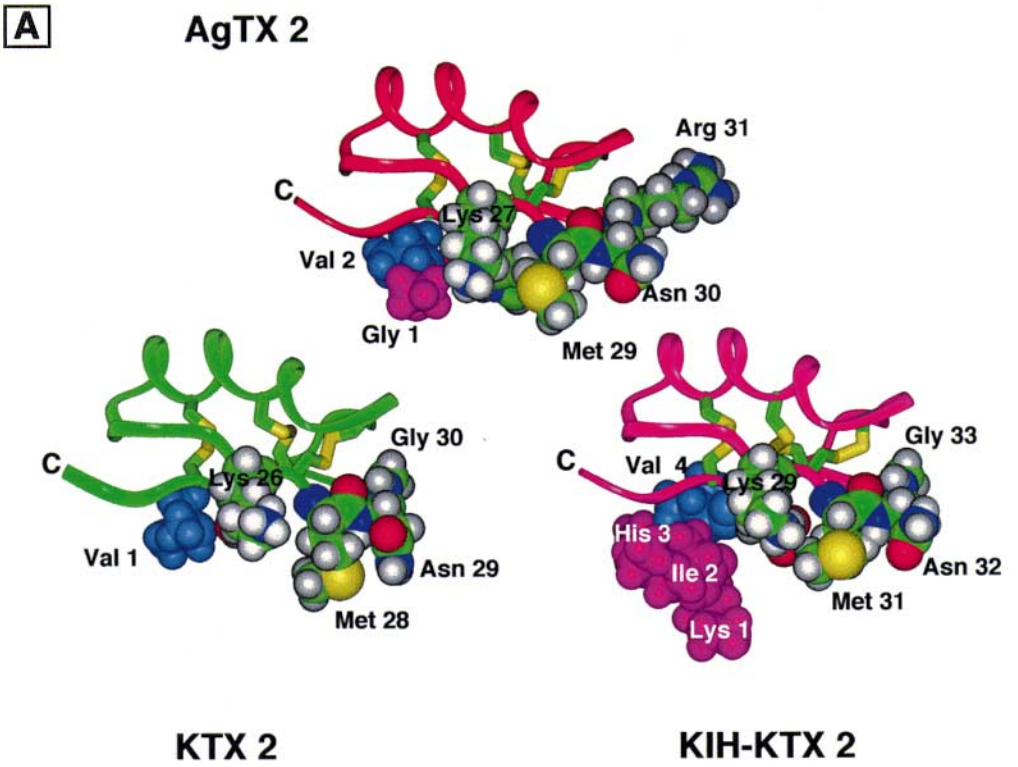

B

AgTX 2	GVPINVSCTGSPQCIKPCKDAGMRFG**KCMNR**KCHCTPK
KTX 2	VRIPVSCKHSGQCLKPCKDAGMRFG**KCMNG**KCDCTPK
KIH-KTX 2	KIHVRIPVSCKHSGQCLKPCKDAGMRFG**KCMNG**KCDCTPK

Fig. 5. Comparison between the structures of AgTX2, KTX2, and KIH-KTX2. A: Ribbon models of AgTX2, KTX2, and KIH-KTX2, obtained by homology modelling with MODELLER. Some residues are displayed as space-filling atoms: residues AgTX2 1–2, KTX2 1, and KIH 1–4 (with the additional residue 1 of AgTX2 and the three additional residues of KIH in magenta) and also residues AgTX2 27–31, KTX2 26–30, and KIH-KTX2 29–33, believed to be important for toxin binding. B: Amino acid sequences of AgTX2, KTX2, KIH-KTX2. Additional residues (in comparison with the N-terminal of KTX2) are in magenta; the residues displayed as space-filling atoms in A are in bold.

KTX2 and one at 88 kDa corresponding to dimers due to disulphide pairing between two MBP-KTX2 (this was demonstrated by SDS-PAGE and blot of the proteins after reduction by dithioerythritol, not shown). As MBP-KTX2 contained six more positive charges than MBP, the three different proteins could be easily purified by HPLC on an anion exchange DEAE-TSK column (data not shown). The MBP-KTX2 constituted 35% of the total affinity-purified proteins, thus about 5–7 mg of fusion protein.

3.2. *Enzymatic cleavage of MBP-KTX2 and characterisation of the recombinant toxin*

The effects of buffer composition (with various amounts of or without different ratios of SDS, urea, guanidine chlorohydrate and/or acetonitrile), pH, enzyme/substrate ratio, enzymes from different sources, digestion time and temperature on cleavage were investigated.

3.2.1. Cleavage of constructions 1 and 2 with factor Xa. Factor Xa was totally unable to cleave MBP-KTX2 under any conditions (Fig. 3A). MBP-KIH-KTX2 was treated with factor Xa and the products purified by HPLC (not shown). Two protein fractions were obtained and their sequences determined. The cleavage (50–70% according to the experimental conditions) was after a GR encoded by the oligonucleotide in the *Bam*HI site of the polylinker (at a sequence ...SSSVPGR/GSIEGRKIH-KTX2), thus giving a KTX2 with nine additional residues at the N-terminus (rGSIEGRKIH-KTX2). Some cleavage (10%) occurred at the factor Xa site. A fraction corresponding to a recombinant KIH-KTX2 (KTX2 with three additional residues at the NH_2-terminal end, thus called rKIH-KTX2) eluted within a retention time of 21 min.

3.2.2. Cleavage of construction 3 with enterokinase. 25–30% of the fusion protein was cleaved. The best recovery yield was obtained with the enterokinase from Biozyme, at pH 8.1

and at 26°C for 24 h, with an enzyme/substrate ratio of 15%. In all cases, cleavage was totally inhibited by SDS, urea and guanidine chlorohydrate, but increased by addition of acetonitrile (10% v/v). So, 0.15–0.30 mg/l of culture is expected. rKTX2 was purified by HPLC at a retention time of 20 min, corresponding to that of the natural KTX2 (Fig. 3B). Its N-terminal sequence (position 1–10) was determined three times after three different cleavages and was as expected. A molecular mass of 4022.8 Da was obtained by electrospray mass spectrometry, in accordance with the molecular mass of 4021.6 Da previously found for native KTX2 and with the expected theoretical mass of 4021.7 Da calculated from amino acid composition and sequence data. Purified rKTX2, rKIH-KTX2, rGSIEGRKIH-KTX2 and MBP-KTX2 were tested in competition experiments with ^{125}I-sKTX for binding to rat brain synaptosomes (Fig. 4). They all inhibited the binding of ^{125}I-sKTX to its receptor site: rKIH-KTX2 with an IC_{50} of 30 nM, rGSIEGRKIH-KTX2 and MBP-KTX2 with an IC_{50} of 0.1 μM and rKTX2 with an IC_{50} of 30 pM. By intracerebroventricular injection into mice, rKTX2 was found to be fully active (lethal dose=35 ng), but rKIH-KTX2, rGSIEGRKIH-KTX2 and MBP-KTX2 were inactive up to 3.5 μg.

3.3. *Modelling of KTX2 and KIH-KTX2*

Conformational models of KTX2 and KIH-KTX2 were designed by sequence alignment with AgTX2, as sequence identity between KTX2 and AgTX2 is higher than that between KTX2 and KTX. The positions of the six half-cystines were used as topological references. Models of KTX2 and of its mutant KIH-KTX2 were obtained within less than 2 h of Central Processing Unit (CPU) time. They were highly rated in Ramachandran plot and overall PROCHECK tests. Fig. 5 shows the two models and that of AgTX2 for comparison [19].

4. Discussion

To investigate the molecular basis of receptor recognition by the related toxins active on K^+ channels, our laboratory has previously studied structure-activity relationships using chemically synthesised analogues [6,22,23]. The three-dimensional structures of some of these analogues, including KTX(1–37) [13] and P05-NH_2, a peptide active on the apamin-sensitive Ca^{2+}-activated K^+ channel [24], have been solved using 2D ^{1}H-NMR spectroscopy. The truncated KTX(1–37) analogue shows some structural differences with other related K^+ channel blockers. To perform additional structural studies by two-, three- and four-dimensional NMR of ^{13}C-, ^{15}N-labelled toxin, it is necessary to develop a bacterial expression system.

We successfully produced KTX2 as a fusion protein in the periplasm of *E. coli*, using the plasmid pMAL-p. The yield of the desired fusion product isolated from the periplasmic space was 5–7 mg/l of culture, giving 300 μg rKTX2 after cleavage from the fusion protein by enterokinase and purification by HPLC. We were unable to recover rKTX2 from a fusion protein containing a factor Xa cleavage site. Attempts at cleavage with Arg C-protease and trypsin were unsuccessful. We suspect a strong interaction between the acidic MBP (Pi=5) and KTX2 (Pi > 10), and this may occlude the recognition site. However, factor Xa cleaved MBP-KIH-KTX2, poorly yielding rKIH-KTX2. Most cleavage events were six amino acid residues upstream of the expected site, but the three additional residues in the N-terminal position of KTX2 seem to improve recognition by the protease.

Heterologous expression of synthetic genes for other small scorpion toxins, like charybdotoxin (ChTX) from *Leiurus quinquestriatus* [25] or margatoxin (MgTX) from *Centruroides margaritatus* [26], has been described in *E. coli*. The fusion proteins produced in the cytoplasm were cleaved by factor Xa after purification and the resulting toxins refolded 'in vitro'. The expression yield of toxin was in some cases 3–4 mg/l. So, the yield of rKTX2 produced in the periplasm is low compared to the amounts of the other toxins active on the K^+ channel obtained by heterologous gene expression in the cytoplasm of *E. coli*. Also, dendrotoxin K (DTX_K) from black mamba, a potent inhibitor of a voltage-dependent K^+ current, and able to compete with ^{125}I-sKTX for its receptor site on rat brain synaptosomes, has been produced as a MBP fusion protein in both the cytoplasm and the periplasm of *E. coli*. The best yield of active toxin (1.5–2 mg/l) was obtained after cleavage by factor Xa of the MBP-DTX_K produced in the periplasm [27].

For the first time, the influence of an additional N-terminal length on the biological activity of a small scorpion toxin active on the K^+ channel was investigated. The ability of ChTX to block IKCa at motor nerve terminals or BKCa (big conductance calcium-activated K^+ channel) of smooth muscles falls dramatically when the N-terminal region is truncated [28,29]. Acetylation or biotinylation of the amino group reduced binding (10-fold) of MgTX to Kv1.3, suggesting the involvement of the N-terminal amino group in the toxin activity [30]. KTX2, like MgTX, exhibits a very high affinity (25 pM) for Kv1.3 channels (Crest, unpublished data). Our results are consistent with those in the literature, since addition of three amino acid residues (KIH) to the N-terminus of KTX2 reduces the activity by a factor of 1000. It is clearly visible (in magenta in Fig. 5) that residues 1–3 of KIH-KTX2 are bulky enough to hinder the Lys^{26} (Lys^{27} in AgTX2) binding to the channel site, or other residues of the β-sheet area involved in the receptor recognition [6,8]. The replacement of Arg^{31} and His^{34} (in AgTX2) by Gly^{30} and Asp^{33} (in KTX2) may account for the lower affinity of KTX2 for Kv1.3 channels: 4 pM for AgTX2 [31] and 25 pM for KTX2 (Crest, personal communication). It has been demonstrated, using analogues of ChTX [8,32,33], KTX [10] and AgTX2 [34], that Lys^{27} can interact with negatively charged residues of the pore and is essential to the activity of the toxins. In KTX, it would interact directly with Asp^{402} (or with the cluster of four Asp^{402}s) of the Kv1.3 channel [10]. Also, the binding affinity of AgTX2 to the Shaker K^+ channel may depends on Arg^{24} and Arg^{31} and the mobility of their side chains may facilitate the formation of the toxin-receptor complex [34,19]. All published toxin-receptor interactions support the existence of a shallow vestibule at the external entrance to the pore: the width of the Kv1.3 vestibule is estimated to be 28–34 Å [10] and that of the Shaker vestibule 22–30 Å [34]. Additional N-terminal residues of rKIH-KTX2 may also increase the contiguous surface area thought to be projected into the mouth of the channel, precluding multiple contacts between the vestibule and the toxin. However, the addition of a longer fragment to the N-terminus of KTX2, as is the case for rGSIEGRKIH-KTX2, did not greatly decrease the activity. The competition between ^{125}I-

sKTX and MBP-KTX2 for the KTX binding site on rat brain synaptosomes indicates that the residues involved in the interaction between KTX2 and its receptor are still accessible.

Acknowledgements: We gratefully thank Dr Andrej Sali who kindly provided MODELLER.

References

[1] Strong, P.N. (1990) Pharmacol. Ther. 46, 137–142.
[2] Miller, C. (1995) Neuron 15, 5–10.
[3] Pongs, O. (1993) Trends Pharmacol. Sci. 14, 435.
[4] Chandy, K.G. and Gutman, G.A. (1993) Trends Pharmacol. Sci. 14, 434.
[5] Crest, M., Jacquet, G., Gola, M., Zerrouk, H., Benslimane, A., Rochat, H., Mansuelle, P. and Martin-Eauclaire, M.-F. (1992) J. Biol. Chem. 267, 1640–1647.
[6] Romi, R., Crest, M., Gola, M., Sampieri, F., Jacquet, G., Zerrouk, H., Mansuelle, P., Sorokine, O., Van Dorsselaer, A., Rochat, H., Martin-Eauclaire, M.-F. and Van Rietschoten, J. (1993) J. Biol. Chem. 268, 26302–26309.
[7] Laraba-Djebari, F., Legros, C., Crest, M., Céard, B., Romi, R., Mansuelle, P., Jacquet, G., Van Rietschoten, J., Gola, M., Rochat, H., Bougis, P.E. and Martin-Eauclaire, M.-F. (1994) J. Biol. Chem 269, 32835–32843.
[8] Park, C.-S. and Miller, C. (1992) Biochemistry 31, 7749–7755.
[9] Goldstein, S.A.N., Pheasant, D.J. and Miller, C. (1994) Neuron 12, 1377–1388.
[10] Aiyar, J., Withka, J.M., Rizzi, J.P., Singleton, D.H., Andrews, G.C., Simon, M., Dethlefs, B., Lee, C.-L., Hall, J.E., Gutman, G.A. and Chandy, K.G. (1995) Neuron 15, 1169–1181.
[11] Gross, A. and McKinnon, R. (1996) Neuron 16, 399–406.
[12] Bontems, F., Roumestand, C., Gilquin, B., Menez, A. and Toma, F. (1991) Science 254, 1521–1523.
[13] Fernandez, I., Romi, R., Szendeffy, S., Martin-Eauclaire, M.-F., Rochat, H., Van Rietschoten, J., Pons, M. and Giralt, E. (1994) Biochemistry 33, 14256–14263.
[14] Bougis, P.E., Rochat, H. and Smith, L.A. (1989) J. Biol. Chem. 264, 19259–19265.
[15] Sambrook, J., Fritsch, E.F. and Maniatis, T. (1989) Molecular Cloning: A Laboratory Manual, Cold Spring Harbor Laboratory, Cold Spring Harbor, NY.
[16] Sanger, F., Nicklen, S. and Coulson, A.R. (1977) Proc. Natl. Acad. Sci. USA 74, 5463–5467.
[17] Riggs, P. (1990) in: Current Protocols in Molecular Biology (Ausubel, F.M. et al., Eds.), Greene Associates/Wiley Interscience, New York.
[18] Sali, A. and Blundell, T.L. (1990) J. Mol. Biol. 234, 779–815.
[19] Krezel, A.M., Kasibhatla, C., Hidalgo, P., McKinnon, R. and Wagner, G. (1995) Protein Sci. 4, 1478–1489.
[20] Laskowski, R.A., MacArthur, M.W., Moss, D.S. and Thornton, J.M. (1993) J. Appl. Crystallogr. 26, 283–291.
[21] Granier, C., Novotny, J., Fontecilla-Camps, J.-C., Fourquet, P., El Ayeb, M. and Bahraoui, E. (1989) Mol. Immunol. 26, 503–513.
[22] Sabatier, J.M., Zerrouk, H., Darbon, H., Mabrouk, K., Benslimane, A., Rochat, H., Martin-Eauclaire, M.-F. and Van Rietschoten, J. (1993) Biochemistry 32, 2763–2770.
[23] Sabatier, J.M., Fremont, V., Mabrouk, K., Crest, M., Darbon, H., Rochat, H., Van Rietschoten, J. and Martin-Eauclaire, M.-F. (1994) Int. J. Peptide Protein Res. 43, 486–495.
[24] Meunier, S., Bernassau, J.M., Sabatier, J.M., Martin-Eauclaire, M.F., Van Rietschoten, J., Cambillau, C. and Darbon, H. (1993) Biochemistry 32, 11969–11976.
[25] Park, C.-S., Hausdorff, S.F. and Miller, C. (1991) Proc. Natl. Acad. Sci. USA 88, 2046–2050.
[26] Garcia-Calvo, M., Leonard, R.J., Novick, J., Stevens, S.P., Schmalhofer, W., Kaczorowski, G.J. and Garcia, M.L. (1993) J. Biol. Chem. 268, 18866–18874.
[27] Smith, A.L., Lafaye, P.J., La Penotiere, H.F., Spain, T. and Dolly, O. (1993) Biochemistry 32, 5692–5697.
[28] Harvey, A.L., Vantapour, H., Rowan, E.G., Pinkasfeld, S., Vita, C., Menez, A. and Martin-Eauclaire, M.-F. (1993) Toxicon 33, 425–436.
[29] Giangiacomo, K.M., Sugg, E.E., Garcia-Galvo, M., Leonard, R.J., McManus, O.B., Kaczorowski, G.J. and Garcia, M.L. (1993) Biochemistry 32, 2363–2370.
[30] Bednareck, M.A., Bugianesi, R.M., Leonard, R.J. and Felix, J.P. (1994) Biochem. Biophys. Res. Commun. 198, 619–625.
[31] Garcia, M.L., Garcia-Calvo, M., Hidalgo, P., Lee, A. and Mac Kinnon, R. (1994) Biochemistry 33, 6834–6839.
[32] Goldstein, S.A.N. and Miller, C. (1993) Biophys. J. 65, 1613–1619.
[33] Stampe, P., Kolmakova-Partensky, L. and Miller, C. (1994) Biochemistry 33, 443–450.
[34] Hidalgo, P. and McKinnon, R. (1995) Science 268, 307–310.